Development of a window system with acoustic metamaterial for air and noise control

***Gioia Fusaro[1,2], Xiang Yu[1], †Fangsen Cui[1] and †Jian Kang[2,3]**

[1]Institute of High Performance Computing, A*Star, Singapore
[2]Acoustics Group, School of Architecture, University of Sheffield, UK
[3]Institute for Environmental Design and Engineering (IEDE), The Bartlett, University College London, UK

*Presenting author: gfusaro1@sheffield.ac.uk

† Corresponding author: cuifs@ihpc.a-star.edu.sg and j.kang@ucl.ac.uk

Abstract

To improve window performances in reducing noise and allowing for air exchange, most current approaches focus on techniques such as double glazed and ducted designs, generally leading to bulky designs, visually non-optimised, and with narrow-banded frequency. In this research, window systems based on acoustic metamaterials (AMMs) are developed, and both natural air ventilation and acoustic performances are evaluated. The systems incorporate bistable auxetic metamaterials and acoustic origami metacage designs which are particularly interesting for their reconfigurable and deployable nature. Several design cases with different design features are examined, and a specific design is then selected for a parametric analysis using Finite Element Method (FEM) aiming to optimise the acoustical performance. It is demonstrated that significant improvement in acoustic performance can be obtained in terms of Transmission Loss (TL). The use of AMMs could lead to designs with manifold merits over traditional windows, including compact size with deployability, easy reconfigurability and installation, and thus paving new direction in ventilation window design.

Keywords: Acoustic metamaterials, Ventilation windows, FEM, auxetic metamaterials, Transmission Loss.

1. Introduction

Conventional acoustic techniques allow controlling sound wave propagation for a limited range of frequency, due to the device shape and bulky configuration (1,2). Metamaterials can be very versatile thanks to its advantages in acoustic properties related to its physical size (3,4). Two specific kinds of metamaterials are particularly interesting from the geometrical point of view: origami metamaterials and bistable auxetic metamaterials. The first metamaterial changes the spatial and the acoustic range of efficacy, while assuming different physical sizes by folding. The second metamaterial has the capacity of keeping a permanent, consistent volume, which may allow openings thanks to their well-known negative Poisson's ratio (5,6). Recent studies have associated such techniques with acoustic performances for mechanical devices improvement (7,8). Actual research is still seeking a significant impact on the combination of noise reduction and natural ventilation, in addition to architectonical sustainable solutions (9).
This study presents a novel acoustic design approach based on two acoustic metamaterials, which enable the natural air ventilation while reducing noise transmission significantly. The two mechanisms (origami and auxetic) are applied to already tested acoustic structure to increase the dynamicity in noise reduction and ventilation capacity (9). A metacage will be implemented by origami system, while a metasurface will be implemented with an auxetic mechanism. These designs allow expansion and compression of the geometries, which surround

(Design 1) or face (Design 2) a sound source. Finite Elements Method (FEM) simulations are performed with a frequency range between 100 and 5000 Hz, in order to attest the effectiveness of the designs. In the first case, two extreme configurations are tested (folded and unfolded configuration). The possibility of using a transparent material to realise both the models give hints for also achieving natural lightning.

2. Methodology

2.1. *Geometrical settings*

FEM simulation is employed to investigate the acoustic characteristics of both models. The boundary conditions and simulation set-ups are detailed in this section.
Two design models are proposed to enable noise reduction and natural ventilation between two separate spaces. For the origami metamaterial (Design 1) the acoustic performance is tested with a monopole sound source in the inside of the mechanism, aiming to screen the radiation towards the outer space. In the bistable metasurfaces (Design 2) the acoustic mechanism works with a surface sound source facing the structure which reduces noise propagation towards space behind it. In both cases, the sound wave and the air are meant to pass through a duct characterised by a number of cavities connected to it. This mechanism is supposed to create a resonance effect and influence significantly the sound wave propagation and so also the TL. In Design 1, the duct system is followed by apertures on the edges of the origami starred points (See Figure *1*). The origami metacage has two different configurations, folded and unfolded, which are both tested through the numerical method to evaluate their acoustic performances. In Design 2, the air and sound wave passes from one space to the other through the openings that are created from the negative Poisson's ratio displacements. As in the previous case, the openings are supported acoustically from a certain number of cavities, which in this case, connect the opening, as shown in Figure 2. Two configurations are tested for Design two. A different rotation angle characterises them as10° and 5°, so that the aperture towards which the cavities face is wider accordingly.

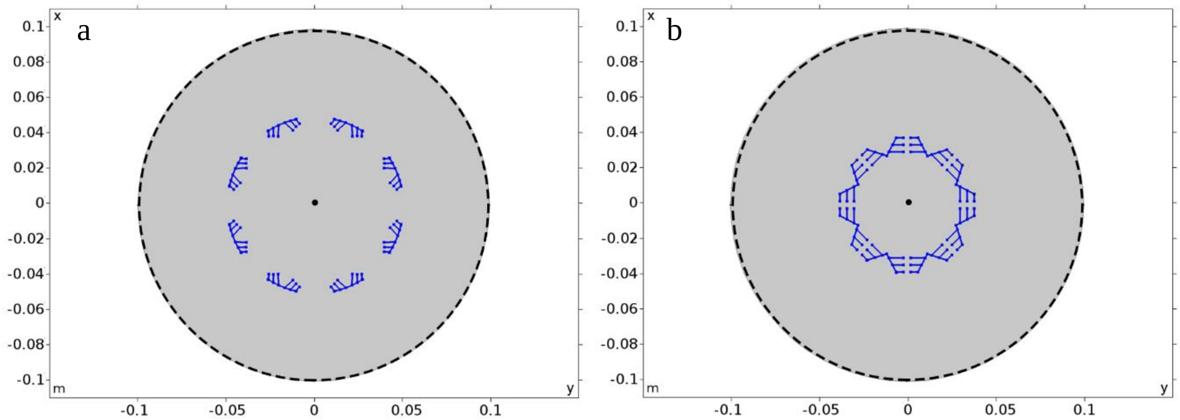

Figure 1. Geometrical configurations of Design 1 unfolded (a) and folded (b) and boundary conditions: central point source, interior sound hard boundaries (blue), and cylindrical free wave radiation (dashed line).

About the geometry in Design 1, it is mainly composed of a deployable system that can achieve two configurations: folded and an unfolded. Indeed, the origami structure allows the valley and mountain folds to go from eight points star shape (with 0.025 m length of each point's side) to a circular shape of 0.256 m diameter. Internally, each point is characterised by an opening 0.052 m each long (52% of perforation ratio of the entire boundary structure) and two cavities with

0.008 m depth created by three layers built starting from the perimeter surface of the metacage. These layers are modelled so they can leave at the centre of the point a resulting duct width 0.008 m which allows the air and acoustic wave to flow freely. When they turn with the structure to assume the unfolded configuration, they have direction perpendicular to the centre with an angular difference of +30° (see Figure 1).

Design 2 is an auxetic metasurface generated from the coupling of two layers, each one made by the repetition and connection of 4x4 basic squared units (each one 0.01 m^2 wide and 0.02 m thick). Figure 2 shows how this unit is repeated and connected with the others through hinges applied on the four edges of each one. From the negative Poisson's ratio displacements, apertures are generated in between the units, which allow the air and sound wave propagation to pass through them. This lead to an opening ratio of 30% for the 10° configuration and of 15% for the 5° one. Each opening has a 50% of perimeter surface removed to allow the resulting cavities to work as a resonator (see Figure 2). Design 2 is characterised by two layers (so four cavities facing the aperture, two per two of the blocks composing it). The openings which result from the Negative Poisson's ratio effect are 10° and 5° wide (see Figure *2*a-c), due to each block rotation (see Figure 2). About the cavities, a further investigation on both Design 1 and 2 is done afterwards, involving the relationship between TL and scale changing of both the models. For Design 1two bigger model are analysed, having respectively 0.4 and 0.8 m diameter in the folded configuration (the original one is 0.2 m). While thickness changing is done on Design 2 to investigate if a 4-layer or 8-layer model (so for a total metasurface thickness of 0.08 or 0.16 m) would affect TL.

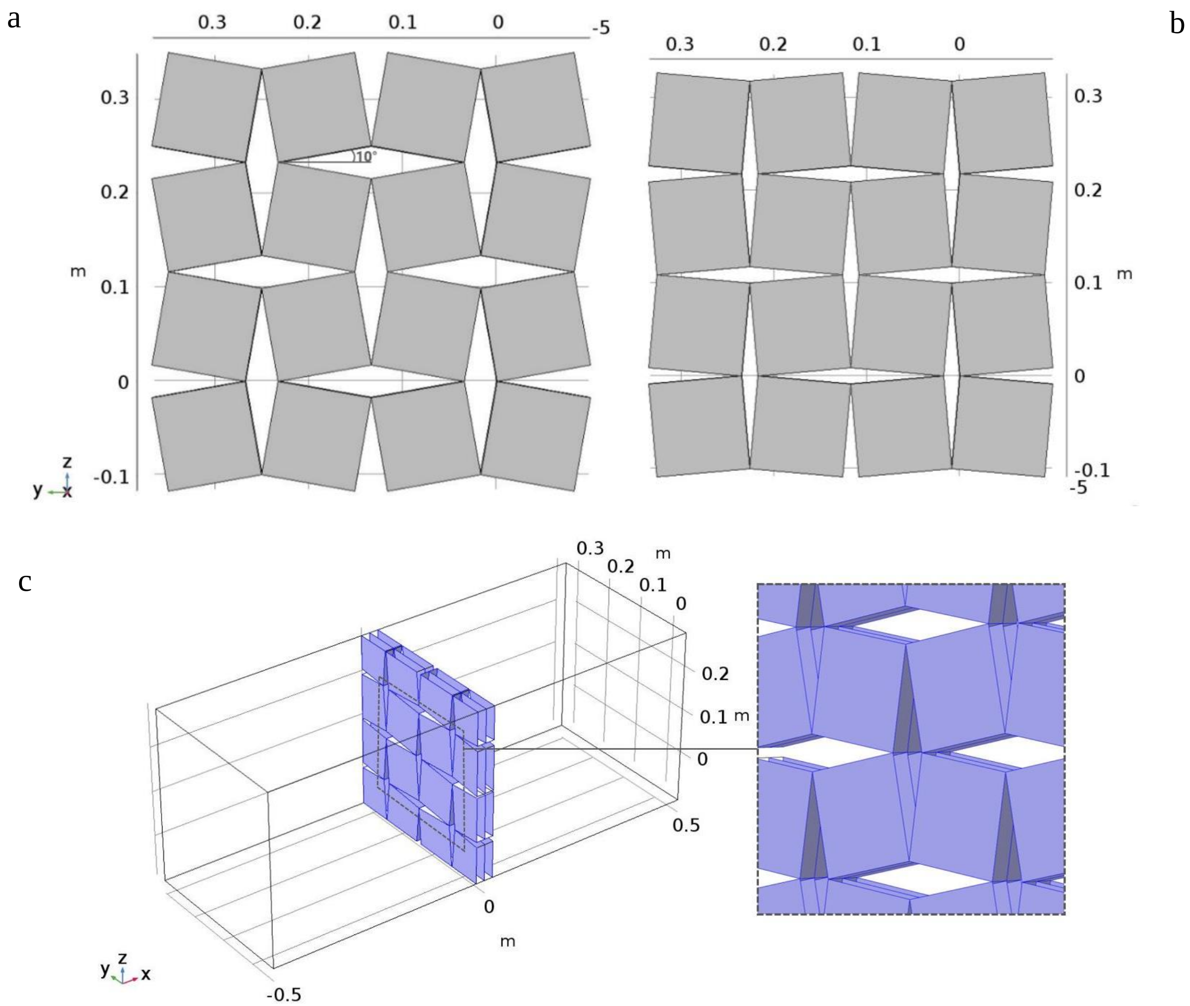

Figure 2. Geometrical configurations of Design 2, frontal view of 10° configuration (a) and 5° configuration (b). Schematic of interior sound hard boundaries, highlighted in blue (c).

2.2. *Boundary Conditions and Study Settings*

The Acoustics module of a commercial FEM software, Comsol Multiphysics, is used to implement the numerical model. For Design 1, a monopole point source is placed at the centre of the origami metacage with volume flow rate is 0.01 m^2/s. At the outer boundary, cylindrical wave radiation is defined to simulate free outgoing waves without reflection. The simulation domain is filled with air, where air density and sound speed at room temperature are used. The walls of the metacage and material cells are set as interior sound hard boundaries, as depicted in Figure 1. Sound transmission through walls of the metacage and possible viscous-thermal effect in the narrow resonator channels are neglected in this study. In Design 2, a plane wave radiation is applied to one of the ends of the 3D boundary volume (incident pressure = 1 Pa). This is a parallelepiped centred with the analysed geometry, having a length of 1 m (x-axis), and a width and depth of 0.38 each (y and z-axis). The opposite end of the boundary volume is characterised with air impedance.

For Design 1, the TL is calculated mathematically within the simulation software, from the averaged SPL at the outlet boundary (dashed line in Figure 1) and the monopole source SPL (=130 dB), to compare the acoustic response in the unfolded and folded state. In Design 2, TL is calculated by the reduction of sound power through the metamaterial interface (in decibel). An increase in the TL curve will thus indicate less efficient sound transmission because sound energy is more confined in the two systems (Design 1 and 2). The mesh size is determined according to the FEM criterion, where at least six nodes are used to simulate a wavelength in air. The dimensions and the complexity of the geometric problems have defined two different frequency ranges of application. So for Design 1, to reach 5000 Hz, the maximum allowed element size is thus 343/6/5000=0.0114 m. Indeed, the study is a frequency domain analysis from 100 Hz to 5000 Hz with a step size of 10 Hz. The meshes characterisation of Design 2 instead, has a maximum allowed element size of 343/6/3000=0.0114 m. Although this model results very complex and, since the convergence of results is proved, simplification is needed. So the maximum allowed element size is increased at 343/6/2000=0.0285 m. The study has a frequency domain that goes from 100 Hz to 3000 Hz with a step size of 10 Hz. In the results, the TL and SPL distribution are shown linearly and superficially within the simulation frequencies.

2.3. *Parametric studies*

The acoustic effectiveness of different metamaterials, is tested through a parametric study in both models. The 2D parameters, ‘cavities thickness’ and ‘duct width’, took in consideration three configurations for the first one (a= 0.006-0.008-0.010 m) and three for the second one (b= 0.006-0.008-0.010 m). In Design 1 each side has two cavities positioned towards the centre (upper section and lower section), delimited by layers which start from the sides and extend towards the middle of it for respectively 0.008 m, 0.012 m, and 0.016 m, and cavities width as 0.08 m (see Figure 3). In Design 2, the parametrization is performed with straight sides and geometry defined by cavities width and layers length. In this case, the layers’ length is set the same for all respectively 0.04 m, 0.06 m, and 0.08 m, and cavities width as 0.01 m, 0.02 m, and 0.03 m (see Figure 3). (see Figure 3). The parametrisation is set to see if there are any interesting correlations between the cavities or the duct’s width and the consecutive TL behaviour.

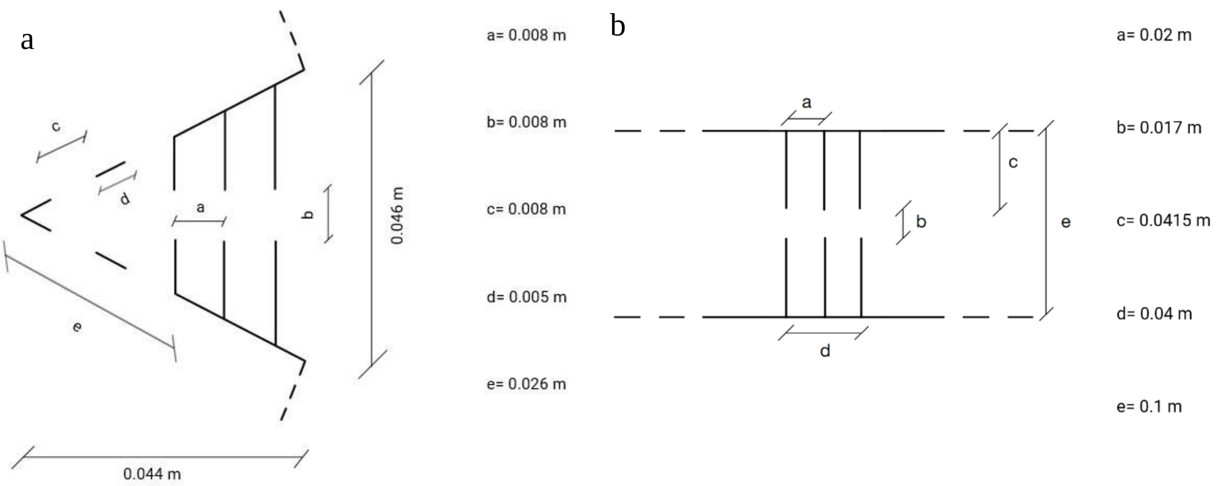

Figure 3. Schematic and dimensions of the metamaterial unit formed in the folded state for Design 1 (a), and of Design 2 (b).

3. Numerical results of Design 1

3.1. *Design 1 (Origami metacage with apertures)*

Figure 4 first shows the simulation results of Design 1 in the folded and unfolded state. The TL is between 8 dB and 30 dB, where some variations can be observed due to the resonance of the circular enclosure. From the TL graph (Figure 4a), both the folded and unfolded configuration effects are analysed. For the folded one the TL reduce significantly at low frequencies (average of 20 dB of TL), while in medium frequency it loose efficacy, and from 2500 Hz to go on, an increasing sinusoidal behaviour starts, with a TL average of 18 dB and a TL peak of 22 dB at 3900 Hz. Figure 4b and 4c highlight the confinement effect of the SPL at the different TL peak frequencies for both unfolded and folded configurations. In both graphs, it is evident how the unfolded state has a slightly higher acoustic impact on the sound wave confinement.

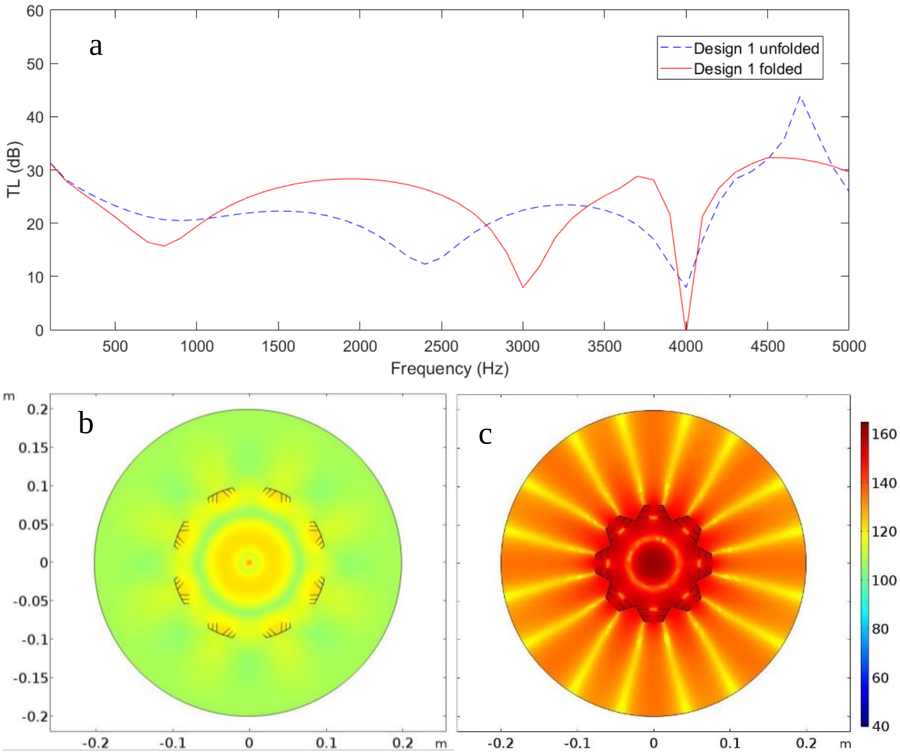

Figure 4. TL (a) and SPL distribution graph for 0.2 m Design 1 at 3000 Hz of the unfolded (b) and 3900Hz of the folded configuration (c).

3.2. *Parametric study on cavities' dimensions ratio*

Figure 5 shows the average behaviours according to two parameters: cavities thickness and duct width. From the nine combinations of the three per three options of two different variables (see schematic in Figure 3): a_1=b_1=0.006 m, a_2=b_2=0.008 m, a_3=b_3=0.01 m. From the results, it is clear that either the cavities or the central duct width change do not affect the acoustic metasurface performance. So the configuration a_2 and b_2 can be set as standard (a_2=b_2=0.008 m) to guarantee a significant sound reduction performance and sufficient ventilation at the same time. Indeed, the acoustic and airwave propagation from the inside to the outside of the metacage and vice versa is guaranteed by the resulted duct of width 0.008 and cavities total thickness of 0.016 m.

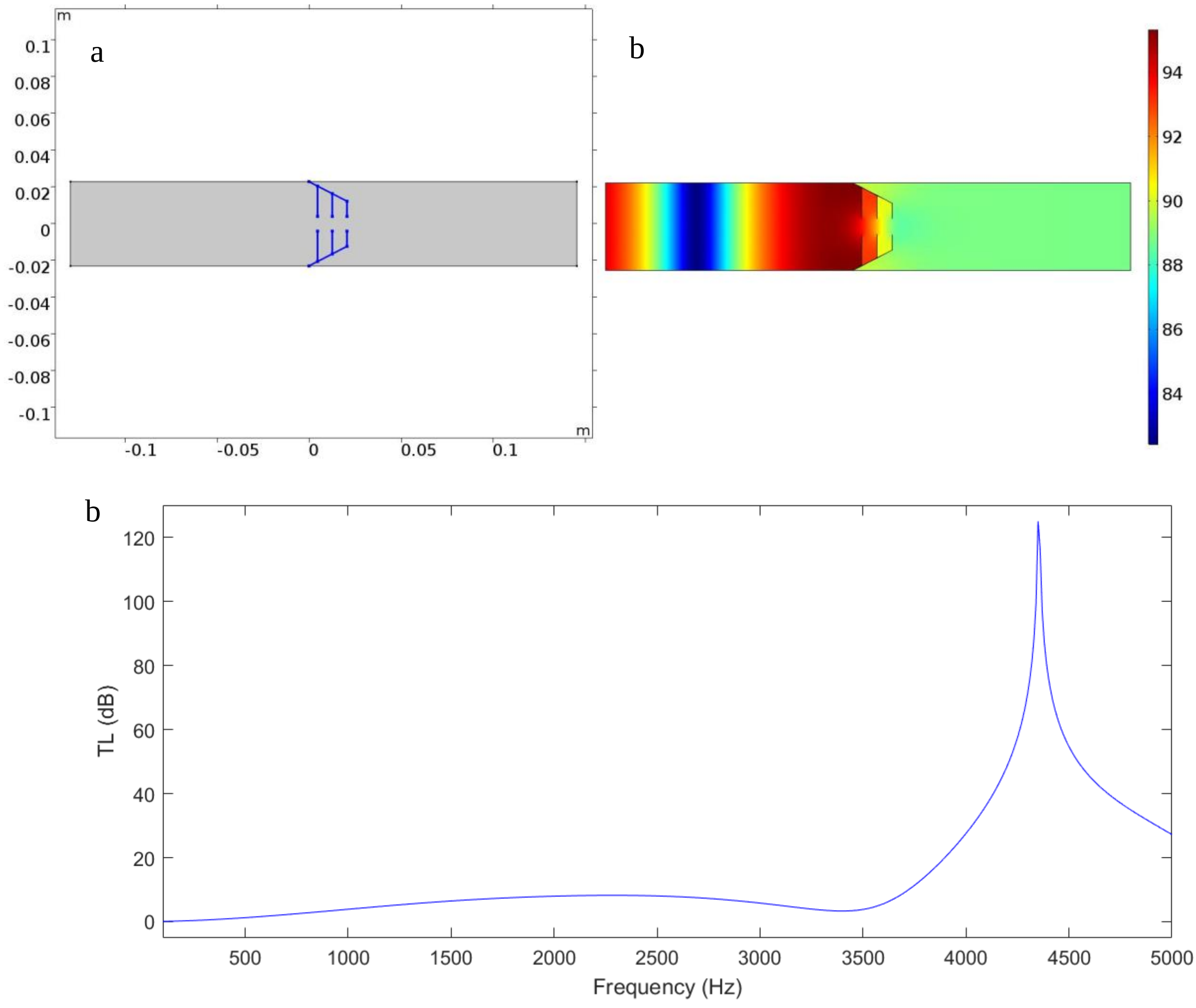

Figure 5. TL Parametrisation for conical duct as the one in Design 1: (a) geometrical setting (internal boundary in blue), (b) SPL distribution at peak frequency 4400 Hz, (c) TL.

3.3. *Comparison of the Different Scaled Models*

The TL increase is correlated with the dimension of the device. For the sake of completeness, wider samples of Design 1 are built and analysed through the same acoustic simulation settings. So results will be presented, comparing the performance of the original model with those of diameter equal to 0.4 and 0.8 m.

From Figure 6, it is clear that, as expected, the increasing of the dimensions (two and four times bigger in this case), causes a shift of the TL peak towards lower frequencies. In particular, for the folded configuration, in the 0.4 m model, the peak is at 4000 Hz (Figure 6) with TL of 83dB. This phenomenon happens consistently and progressively with the increasing of the models,

and it is demonstrated by the other study, with dimensions ten times bigger than the original ones. For the 0.8 m models, the peak is at 2000 Hz where SPL is 89dB.
From Figure 6, the effectiveness of the origami metacage it is demonstrated in this frequency range, and the contribution of the folded configuration in this process is proved.

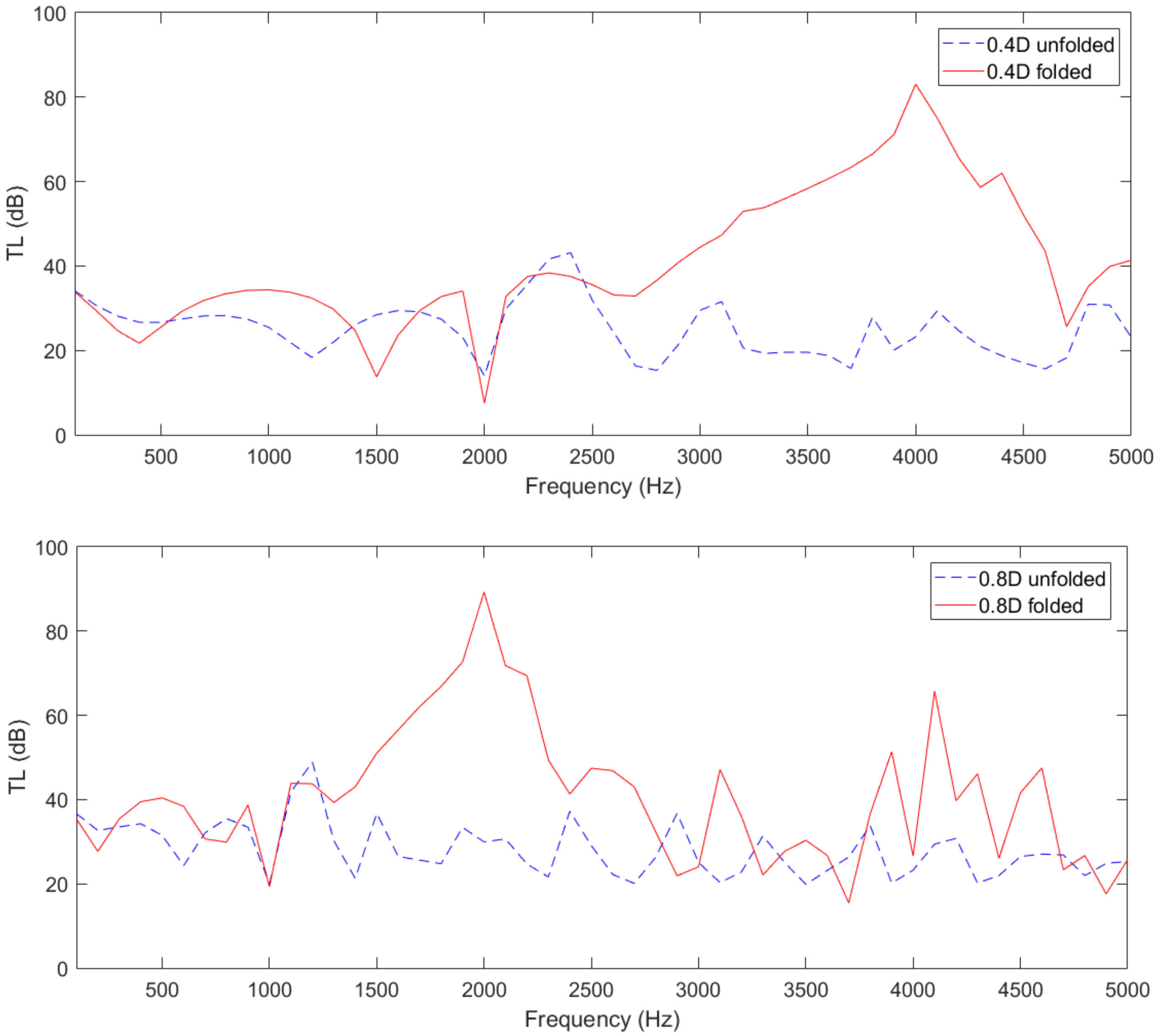

Figure 6. TL comparison of Design 1 (unfolded and folded) with different diameters dimensions (0.2, 0.4, and 0.8 m).

4. Numerical results of Design 2

4.1. *Design 2 (Bistable Auxetic)*

Figure 7 shows the simulation results of Design 2. For the SPL distribution, a slice graph is placed at the middle of the metasurface height, to compare the effect of the two models (Design 1 and Design 2). In both configurations (10° and 5° rotating angles), the TL behaviours are very similar but shifted on lower results for the 10° one. Overall, the TL is between 0 dB and 51 dB, where some variations can be observed due to the resonance of the openings of the cavities composing the duct. The TL has a sinusoidal behaviour at low-medium frequencies (500-1500 Hz, average of 7 dB), while in the upper-medium frequency range (1500-3000 Hz) it increases in efficacy, with a TL average of 23 dB and a TL peak of 51dB at 1700 Hz. Figure 7b highlights the confinement effect of the SPL at the TL peak frequency for both 10° and 5° configurations.

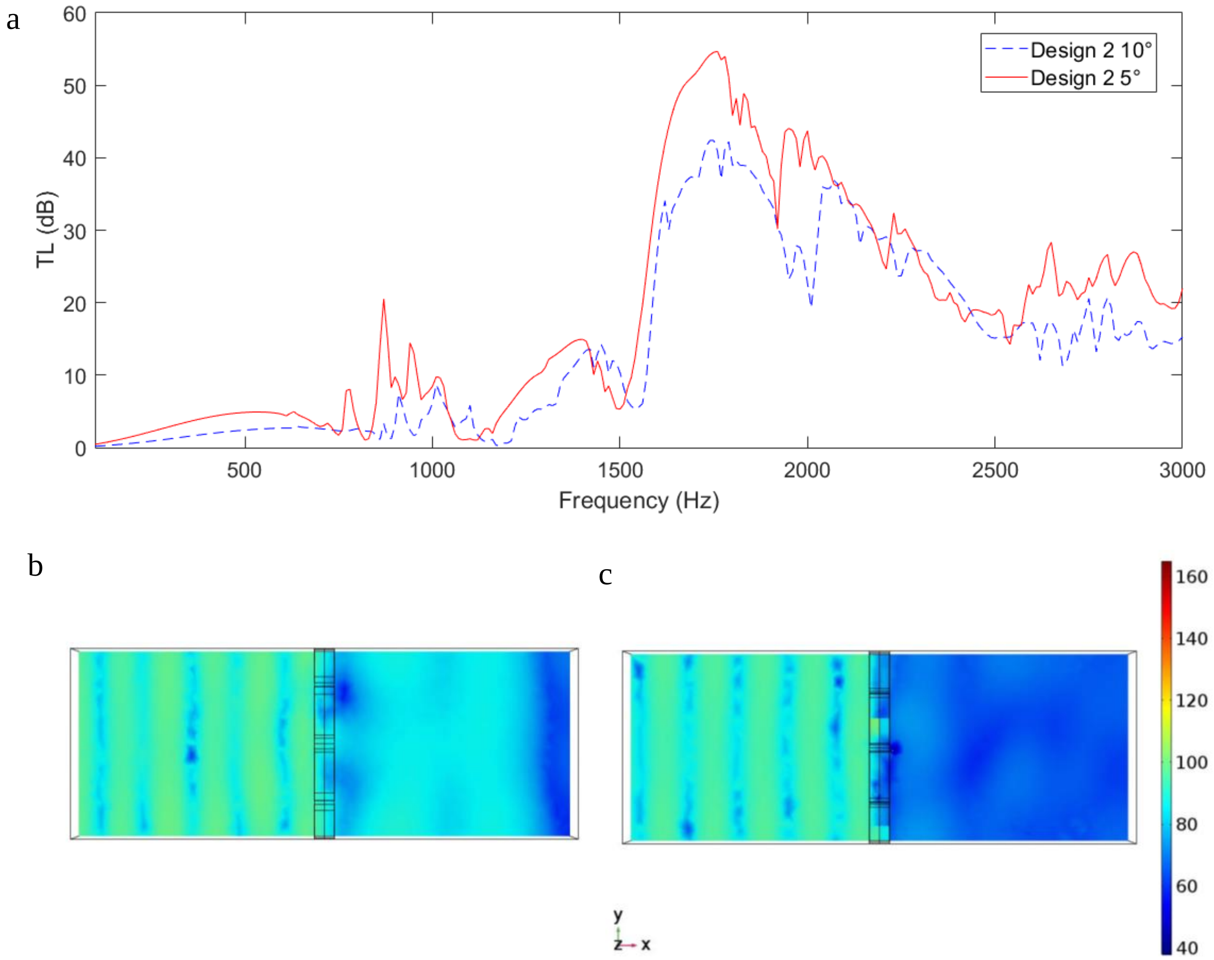

Figure 7. TL (a) and SPL distribution graph for Design 2 10° at 1800 Hz (b) and Design 2 5° at 1700 (c).

4.2. *Parametric study on cavities' dimension's ratio*

Figure 8 shows the average behaviours according to the two variables considered: cavities thickness and duct width. From the nine combinations of the three per three different options (see schematic in Figure 3): a_1=b_1=0.01 m, a_2=b_2=0.02 m, a_3=b_3=0.03 m. From the results, it is clear that either the cavities or the central duct width change do not affect the acoustic metasurface performance. So the configuration a_2 and b_2 can be set as standard (a_2=b_2=0.02 m) to guarantee a significant sound reduction performance and sufficient ventilation at the same time. Indeed, the acoustic and airwave propagation from the inside to the outside of the metacage and vice versa is guaranteed by the resulted duct of width 0.017 and cavities total thickness of 0.04 m.

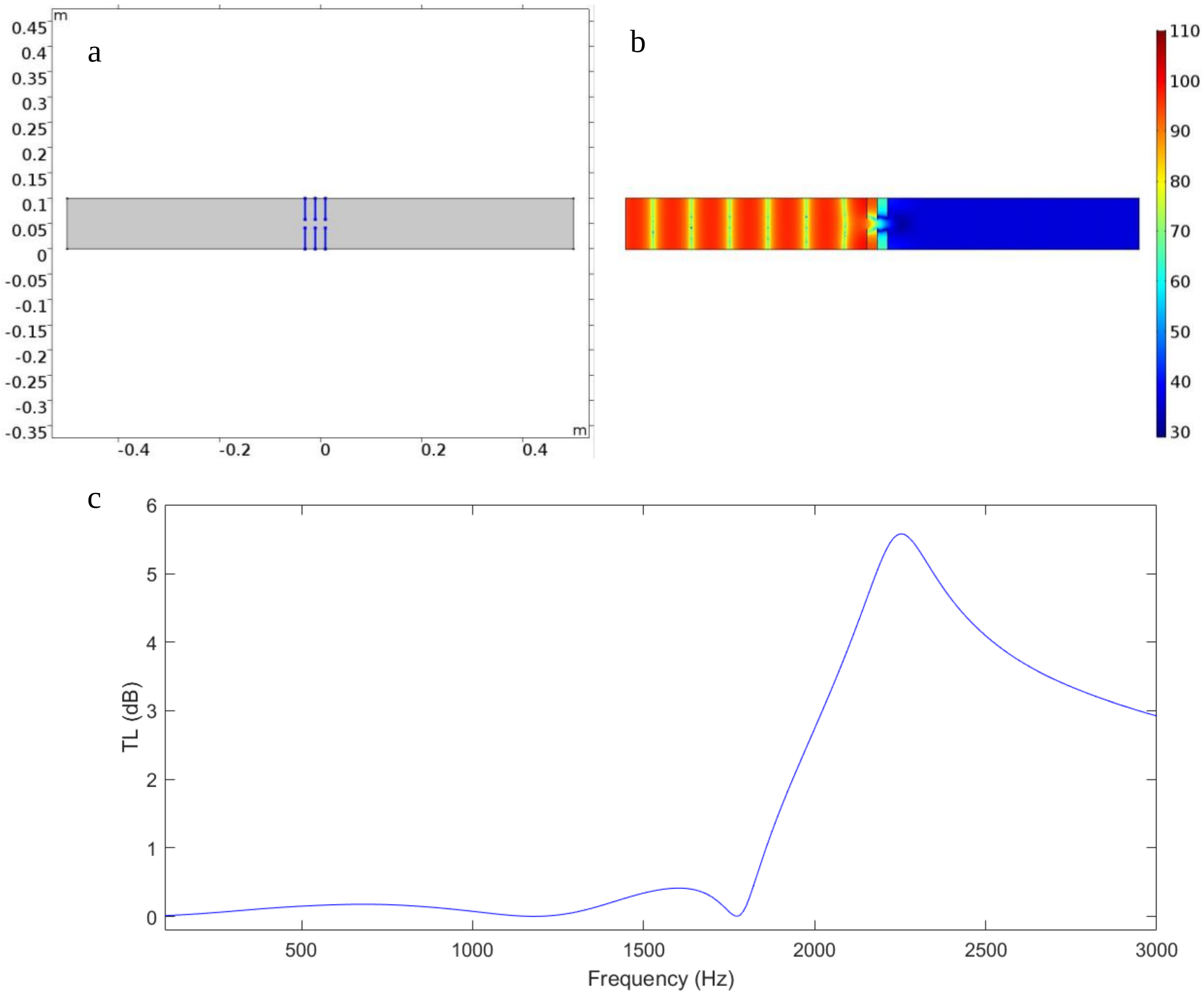

Figure 8. TL Parametrisation for straight duct reproducing the one in Design 2: (a) geometrical setting (internal boundary conditions in blue), (b) SPL distribution at peak frequency 2300 Hz, (c) TL.

4.3. *Comparison of the Different Scaled Models*

Differently from Design 1, the TL increase is not significantly correlated with the dimension of the device. For the sake of completeness, thicker samples of Design 2 are built and analysed through the same acoustic simulation settings. The results are presented in Figure 9, comparing the performance of the original model with those of overall thickness equal to 0.08 and 0.16 m. From Figure 9, it is clear that there is no shift of the TL peak while increasing the metasurface thickness. In particular, an interesting result is the different tendency of 10° and 5° configuration. While the TL associated with the first one decreases its amplitude around the peak frequency range (1500-2500 Hz), the second one increase significantly. The peak is always around 1700 Hz, but the amplitude is different. For the four-layer models, the TL peak is indeed 67dB (1760 Hz) for the 5° configuration, and it is averagely 38 dB for the 10° one (much spread and less concentrated than the previous one). The eight-layer model TL peak is lower again for the 10° configuration (averagely 40 dB), while increases with a maximum peak of 77 dB for 5° model at 1740 Hz.

Generally, from Figure 9, the effectiveness of the auxetic metasurface appears not to be connected significantly with the thickness increase. A part from the isolated peak, the graph shows a similar overall behaviour of TL related to the model with 2, 4, and 8 layers of Design 2. This means that, differently from Design 1, a two-layer model might be enough to allow natural ventilation and reduce noise on a broader frequency band.

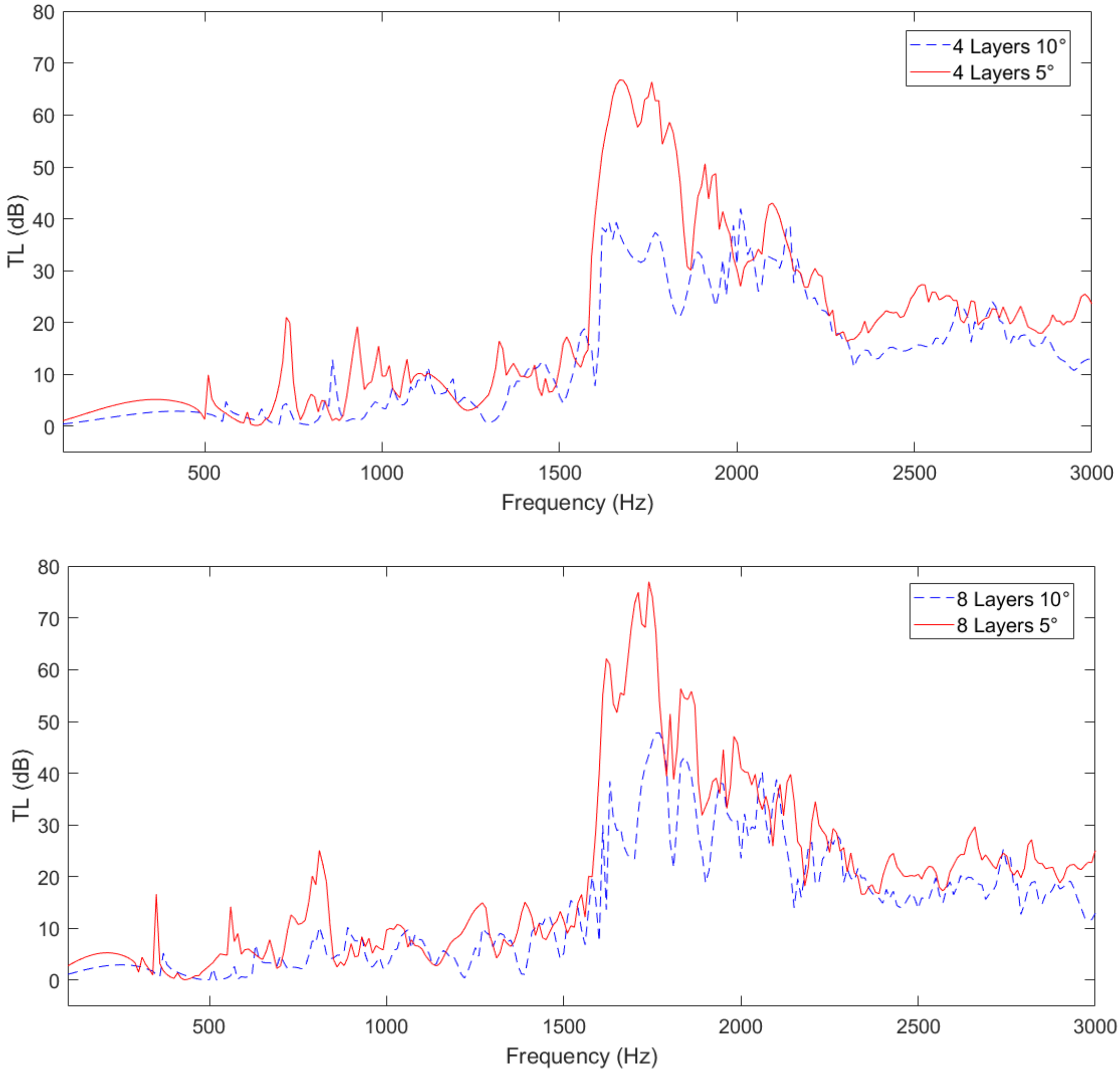

Figure 9. TL comparison of Design 2 (unfolded and folded) with different diameters dimensions (0.2, 0.4, and 0.8 m).

5. Discussion on possible design applications

The main aims of this research are achieved, and further numerical improvement or experimental study on the model will give more completeness to the research. So now new possibilities are open for devices' design which aim noise reduction together with natural ventilation. The proposed geometry may be embedded in a window design. The resulting TL broad peaks of 54, 67, and 77 dB (two, four and eight-layer model) might result of some impact in a situation where the application area is affected by high-level noise. An example for Design 1 could be to embed a system of origami metacage ducts in window frames or using the structure itself with increased width and a transparent back panel to allow also light exchange between two environments. The structure of Design 2 could be used as a transparent panel for windows enclosures. A further parametrisation and validation work will follow to test the actual building feasibility of the prototypes and determine whether the use of transparent materials might affect their performance or allow a new generation of tunable window systems.

6. Conclusions

The acoustic characteristics of the proposed acoustic metamaterials with a unique reconfigurable mechanism have been investigated. Different configurations with specific ventilation designs have been tested to assess the noise reduction and estimate the ventilation volume between the two areas separated by the devices: the inside and the outside for Design 1 (52% of opening ratio) and front and back for Design 2 (from 15% to 30% of opening ratio). Both models show high peaks in the TL due to the effective silencing effect provided by each metamaterial unit in front of the ventilation apertures. In different effective ways, the frequency and bandwidth of the effective region are related to the geometric parameters and scales of the systems. The potential of the proposed devices to be used in ventilation window systems is proved since natural ventilation is possible without any additional element. Better ventilation and noise reduction in the desired frequency range can be achieved by developing further numerical models for optimising the devices in terms of size and shape.

REFERENCES

1. Lam B, Elliott S, Cheer J, Gan WS. Physical limits on the performance of active noise control through open windows. Appl. Acoust. 2018;137:9–17.
2. Kang J, Brocklesby MW. Feasibility of applying micro-perforated absorbers in acoustic window systems. Appl. Acoust. 2005 Jun 1;66(6):669–89.
3. Yu X, Lau S-K, Cheng L, Cui F. A numerical investigation on the sound insulation of ventilation windows. Appl. Acoust. 2017; 117:113–121
5. Yu X, Lu Z, Cheng L, Cui F. On the sound insulation of acoustic metasurface using a sub-structuring approach. J Sound Vib. 2017;401:190–203.
6. Yu X, Fang H, Cui F, Cheng L, Lu Z. Origami-inspired foldable sound barrier designs. J Sound Vib. 2019;442:514–26.
7. Babaee S, Overvelde JTB, Chen ER, Tournat V, Bertoldi K. Reconfigurable origami-inspired acoustic waveguides. Sci Adv. 2016;2(11):e1601019–e1601019.
8. Shen C, Xie Y, Li J, Cummer SA, Jing Y. Acoustic metacages for sound shielding with steady air flow. J Appl Phys. 2018;123(12).
9. Ma G, Sheng P. Acoustic metamaterials: From local resonances to broad horizons. Sci Adv. 2016;2(2):e1501595–e1501595.